Supplementary material for LHCb-PAPER-2021-035

The measurement of A_{CP} is shown in Fig. 1. The measurement of the full set of *CP*-averaged angular observables $\langle S_i \rangle$ can be found in Fig. 2 and Fig. 4 for $D^0 \to \pi^+\pi^-\mu^+\mu^-$ and $D^0 \to K^+K^-\mu^+\mu^-$ decays, respectively. The measured *CP* asymmetries $\langle A_i \rangle$ are shown in Fig. 3 and Fig. 5. Background-subtracted $m(\mu^+\mu^-)$ and $m(h^+h^-)$ distributions can be found in Fig. 6, where the data is corrected for phase-space dependent efficiency variations. Since Fig. 6 does not include systematic uncertainties, it cannot be considered as a measurement of the differential branching fraction.

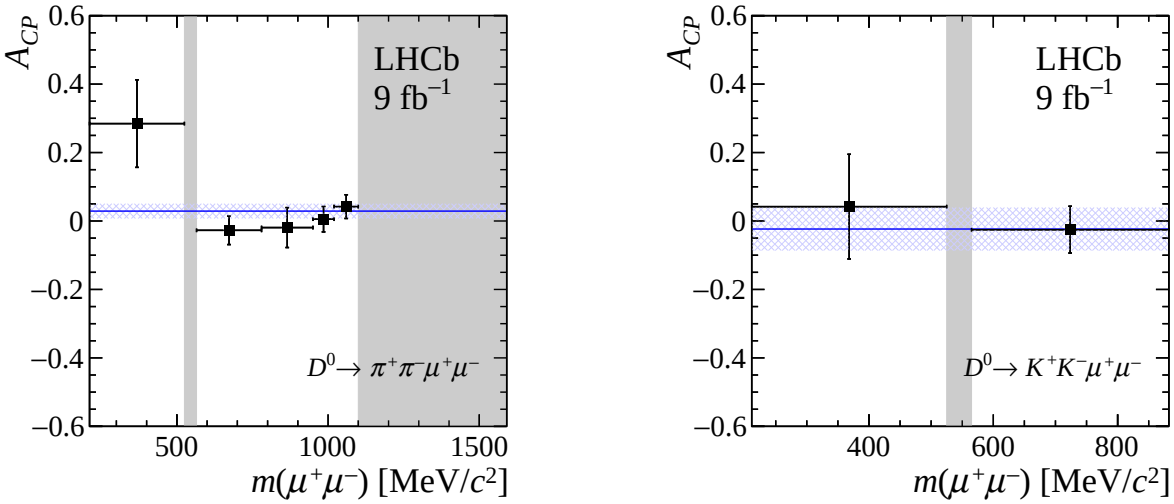

Figure 1: Measurement of A_{CP} in regions of dimuon mass for (left) $D^0 \to \pi^+\pi^-\mu^+\mu^-$ and (right) $D^0 \to K^+K^-\mu^+\mu^-$. No measurement is performed in the regions indicated by the vertical gray bands. The horizontal bands correspond to the measurements integrated in the dimuon mass, including candidates from all $m(\mu^+\mu^-)$ ranges. The uncertainties are the statistical and systematic uncertainties summed in quadrature.

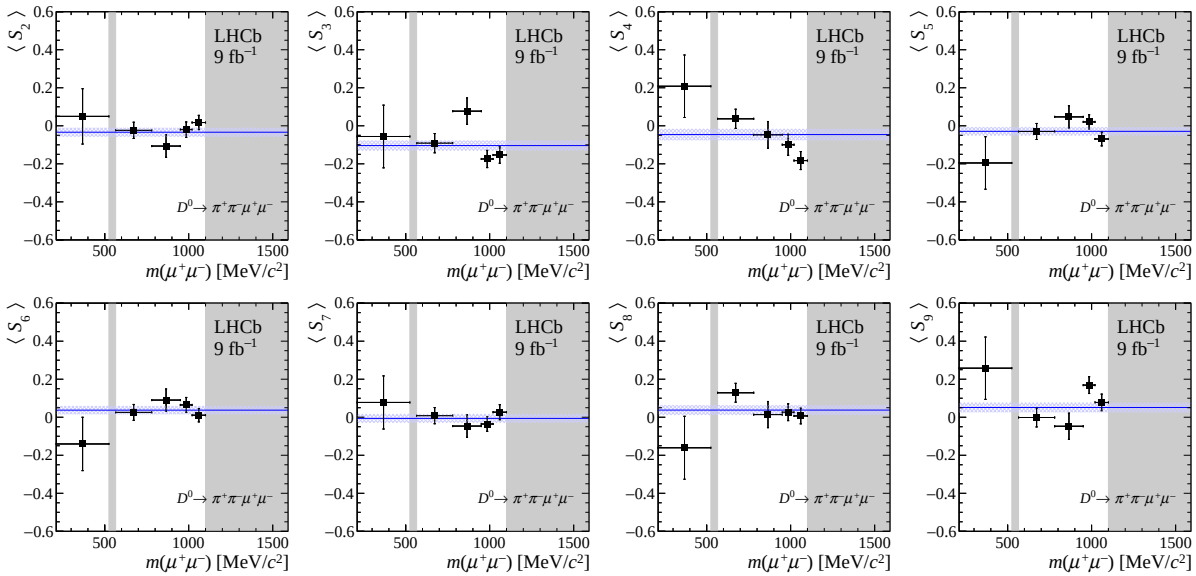

Figure 2: Measurement of *CP*-averaged angular observables $\langle S_i \rangle$ in regions of dimuon mass for $D^0 \to \pi^+\pi^-\mu^+\mu^-$ decays.No measurement is performed in the regions indicated by the vertical gray bands. The horizontal bands correspond to the measurements integrated in the dimuon mass, including candidates from all $m(\mu^+\mu^-)$ ranges. The uncertainties are the statistical and systematic uncertainties summed in quadrature.

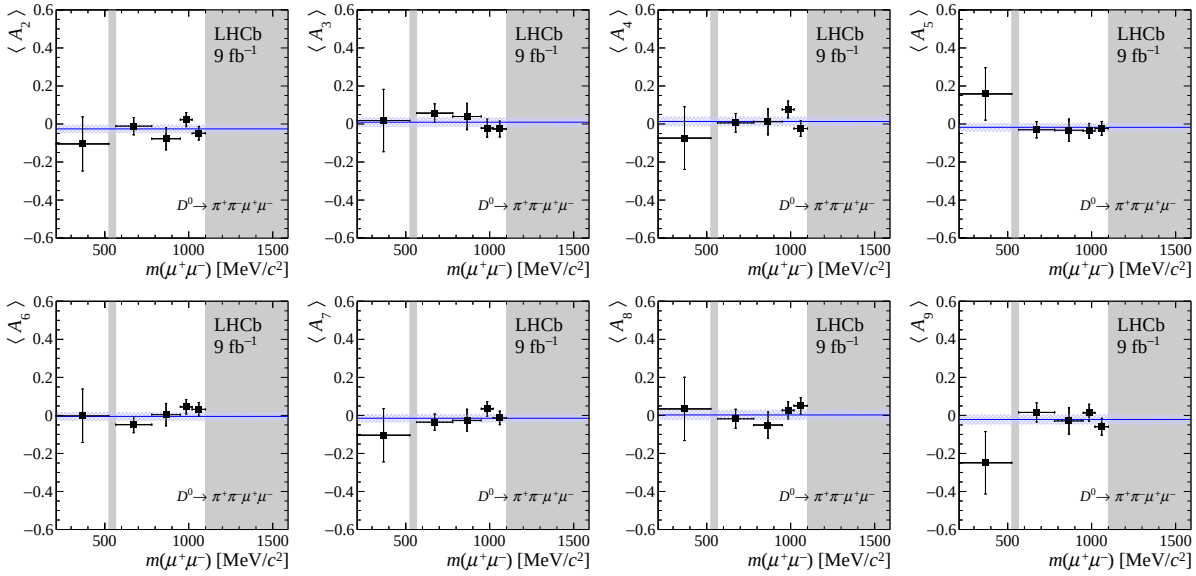

Figure 3: The *CP* asymmetries of angular observables $\langle A_i \rangle$ in regions of dimuon mass for $D^0 \to \pi^+\pi^-\mu^+\mu^-$ decays. No measurement is performed in the regions indicated by the vertical gray bands. The horizontal bands correspond to the measurements integrated in the dimuon mass, including candidates from all $m(\mu^+\mu^-)$ ranges. The uncertainties are the statistical and systematic uncertainties summed in quadrature.

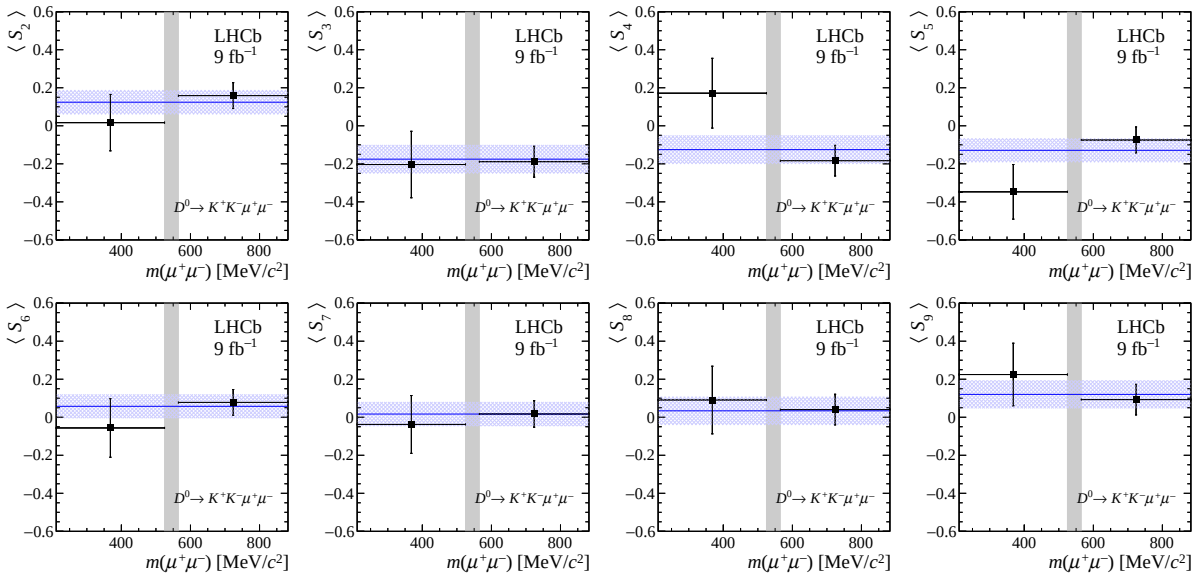

Figure 4: Measurement of *CP*-averaged angular observables $\langle S_i \rangle$ in regions of dimuon mass for $D^0 \to K^+K^-\mu^+\mu^-$ decays.No measurement is performed in the regions indicated by the vertical gray bands. The horizontal bands correspond to the measurements integrated in the dimuon mass, including candidates from all $m(\mu^+\mu^-)$ ranges. The uncertainties are the statistical and systematic uncertainties summed in quadrature.

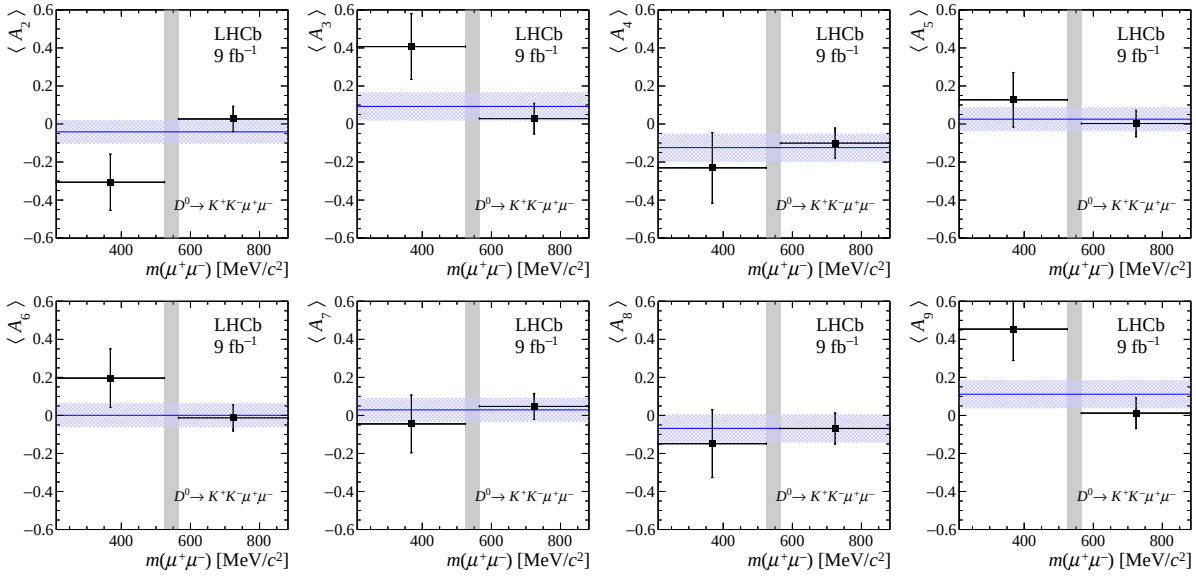

Figure 5: Measurement of *CP* asymmetries of angular observables $\langle A_i \rangle$ in regions of dimuon mass for $D^0 \to K^+K^-\mu^+\mu^-$ decays. No measurement is performed in the regions indicated by the vertical gray bands. The horizontal bands correspond to the measurements integrated in the dimuon mass, including candidates from all $m(\mu^+\mu^-)$ ranges. The uncertainties are the statistical and systematic uncertainties summed in quadrature.

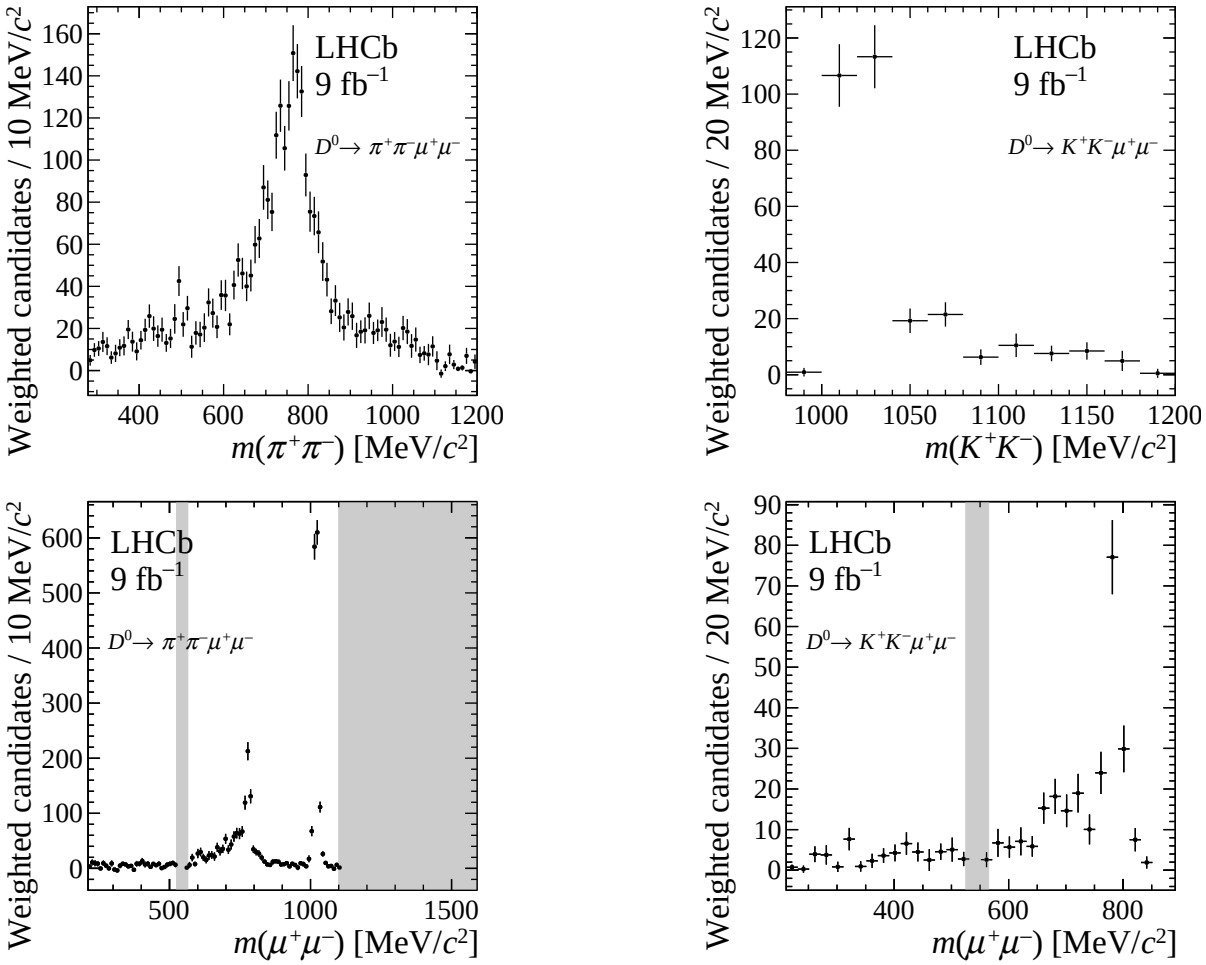

Figure 6: Background-subtracted (top) dimuon-mass and (bottom) dihadron-mass distributions for (left) $D^0 \to \pi^+\pi^-\mu^+\mu^-$ and (right) $D^0 \to K^+K^-\mu^+\mu^-$ decays. The gray shaded areas correspond to the regions where no signal was previously observed and are removed from the plots. The data is corrected for phase-space dependent efficiency variations. The uncertainties are statistical only. Since no systematic uncertainties are included, the plot cannot be considered as a measurement of the differential branching fraction.